




# Magnetic properties and thermal stability of Fe-based amorphous/carbonyl iron soft magnetic composites

Jibiao Shen<sup>1</sup>, Bin Wang<sup>1,\*</sup>, Lingwen Cai<sup>2</sup>, Lidong Liu<sup>2</sup>, Cong Zhang<sup>3</sup>, Bingxing Wang<sup>1,\*</sup> , Yong Tian<sup>1</sup>, Yangdong Yu<sup>2</sup>, Jiangqun Dong<sup>2</sup>, and Guodong Wang<sup>1</sup>

<sup>1</sup> State Key Laboratory of Rolling and Automation, Northeastern University, Shenyang 110819, China

<sup>2</sup> Hengdian Group DMEGC Magnetics Co. Ltd, Hengdian Group Holdings Co Ltd, Dongyang 322100, China

<sup>3</sup> School of Materials Science and Engineering, Anhui University, Hefei 230601, China

**Received:** 13 February 2023

**Accepted:** 22 April 2023

**Published online:**

19 May 2023

© The Author(s), under exclusive licence to Springer Science+Business Media, LLC, part of Springer Nature 2023

## ABSTRACT

In this research, Fe–Si–B/carbonyl iron soft magnetic composites were prepared with the aim of having low magnetic loss and temperature-dependent characteristics. An increase in the carbonyl iron powder content resulted in an increase of saturation magnetization intensity in the Fe–Si–B/carbonyl iron hybrid powder. The presence of carbonyl iron particles improved the coupling between the Fe–Si–B particles, reducing iron loss and enhancing the magnetic permeability of the soft magnetic composites, resulting in excellent magnetic properties even at high frequencies and temperatures. However, when the content of carbonyl iron powder surpassed 25% and reached 40%, its effect on the magnetic performance of the soft magnetic composites decreased.

## 1 Introduction

The rapid development of the power electronics industry has driven the demand for electronic equipment with high frequency, small integration, light weight, and excellent DC superposition characteristics. This has led to a growing need for power magnetic materials that can function under high-frequency transmission conditions, which is crucial for the advancement of ultra-large-scale digital-integrated circuits in high frequency [1, 2]. Soft magnetic composite materials are an integral part of integrated circuits and come in various forms, including FeSi, Mn–Zn ferrite, Fe–Si–B–P–Cu, Fe–Si–B, and Fe–Cu–Nb–Si–B, etc. According to the different properties of

these magnetic powders, they are usually used in different fields. For example, FeSi is mainly used in magnetic cores for filters and inductors. The high-permeability Mn–Zn ferrite material is mainly used in electronic circuits for wideband transformers, pulse transformers, and other fields. The magnetic permeability of Fe–Si–B series amorphous/nanocrystalline alloy powder is lower than the above two soft magnetic materials, but it has the advantages of higher resistivity, high-saturation flux density, etc., which can be used in switching power supply and power inductors. [3–6]. As digital-integrated circuits continue to shrink in size and increase in frequency, soft magnetic composites are facing higher performance demands. The ability to maintain

Address correspondence to E-mail: wangbin@ral.neu.edu.cn; wangbx@ral.neu.edu.cn

low magnetic loss and high magnetic permeability under high-frequency magnetic fields is essential in determining the performance of these materials.

Studies have been conducted on the properties of soft magnetic composites operating at high frequencies  $\geq 1$  MHz [7–9]. Fe–Si–B amorphous composites are popular due to their high-saturation magnetic induction, low high-frequency magnetic losses, and low coercivity [10, 11]. The magnitude of eddy current losses depends on factors such as frequency, amplitude, and shape of the magnetic field, as well as the geometric shape and size of the material. Amorphous metals have lower eddy current losses at high frequencies compared to crystalline metals because of their unique disordered atomic arrangement [12, 13]. However, Under the same molding pressure, the high hardness of amorphous magnetic powder makes the forming of soft magnetic composite materials more difficult than that of iron-nickel and iron-silicon magnetic powders [14]. This leads to strong interaction forces during the pressing process, which affects the performance of the composite material. Increasing the molding pressure decreases the yield, while lowering it decreases the performance of the composite.

In this paper, a novel method for fabricating soft magnetic composites with high-frequency characteristics is proposed. High frequency with low magnetic losses soft magnetic composites were prepared by adding low hardness and small particle size carbonyl iron powder to Fe–Si–B amorphous powder particles. Carbonyl iron powder has the characteristics of small particle size (below 10  $\mu\text{m}$ ). Which is widely used in the manufacture of magnetic materials because of its high magnetic flux rate at high frequency and ultra-high frequency and has an irreplaceable role in the preparation of high-frequency soft magnetic composite materials. The carbonyl iron powder particles with low hardness and small particle size not only play the role of filling the gap during the pressing process of the soft magnetic composite material, but also can effectively improve the cracking phenomenon caused by the large internal stress of the Fe–Si–B amorphous soft magnetic composite material. Specifically, the method produces composites with magnetic loss below 500  $\text{kW}/\text{m}^3$  at a magnetic induction intensity of 20mT and a frequency of 1 MHz.

## 2 Experimental materials and methods

High-frequency soft magnetic composites were prepared using Fe–Si–B amorphous powder as raw material and carbonyl iron powder as additive in this experiment. The Fe–Si–B amorphous powder prepared by the combined water and gas atomization method contains 2.4wt% Si, 3.5wt% B, 0.6wt% C, 0.5wt% Cr, and Fe in balance. BASF's carbonyl iron powder with different mass ratios were added to Fe–Si–B amorphous powders to preparation of soft magnetic composites. By testing the magnetic properties of several groups of soft magnetic composites, the effects of different content of carbonyl iron powder additives on the magnetic losses, permeability, and other properties of soft magnetic composites at high frequency were investigated. The content of carbonyl iron powder additive is 7.7wt%, 14.3wt%, 25.0wt%, and 40.0wt% of Fe–Si–B/carbonyl iron-mixed powder, respectively.

The powder particles were uniformly passivated with 0.2wt% phosphoric acid solution diluted with 10wt% acetone solution, and 2wt% high-temperature-resistant silicone resin diluted with 10wt% acetone solution was used as a binder. The Fe–Si–B/iron carbonyl hybrid powder particles were prepared in long strips by granulation, which is conducive to particle flow, and 0.2wt% aluminum stearate as a lubricant is beneficial to the compression molding of the soft magnetic composite. The soft magnetic composites were molded with a pressure of 1500 MPa, dimensional parameters of 14.00 mm outer diameter, 7.95 mm inner diameter, and annealed to 420 °C for 120 min. After annealing, the magnetic properties such as relative permeability, magnetic loss, and complex permeability were tested by winding 25 turns of insulated copper wire on the surface of the soft magnetic composite.

The particle size distribution of the powder particles was measured by a HELOS&RODOS laser particle size analyzer. X-ray diffractometer was used for phase analysis of powder particles and the morphology of powder particles before and after granulation was photographed by Hitachi s-3000n scanning electron microscope. The hysteresis loops of the powder samples were tested using a LakeShore 7404 vibrating sample magnetometer. The element distribution and valence state of the powder surface were tested by JXA-8530 F PLUS EPMA and thermo scientific K-Alpha + X-ray electron spectrometer,

respectively. The tests on the relative permeability and iron loss of the soft magnetic composites were performed using the IWATSU soft magnetic B-H SY-8219 analyzer from Iwasaki. The complex permeability of the soft magnetic composites was measured by using a WK6500b precision impedance analyzer.

### 3 Results and discussion

The XRD patterns of Fe–Si–B and carbonyl iron powders are shown in Fig. 1a, and the XRD patterns of Fe–Si–B show a typical amorphous state. The particle size distribution of Fe–Si–B amorphous powder and carbonyl iron powder is shown in Fig. 1b. The particle size distribution test results show that the particle size of carbonyl iron is much smaller than that of Fe–Si–B powder, which helps carbonyl iron particles to fill the voids between Fe–Si–B particles effectively. The morphologies of Fe–Si–B amorphous powder and carbonyl iron powder are shown in Fig. 1c and d, and the approximately spherical particles are more conducive to the molding of soft magnetic composites. The particle morphology of the powder after granulation is also shown in Fig. 1e and f. The spherical carbonyl iron powder with small particle size is filled in the gaps between the large particles to act as a lubricating buffer to increase the density and improve the performance of the soft magnetic composite. The EPMA test results of Fe–Si–B/25%wt carbonyl iron hybrid particles after insulation coating are shown in Fig. 2. The phosphoric acid passivation and high-temperature-resistant silicone resin-insulation-coating process can form an insulating layer on the surface of the powder particles, which can effectively reduce the high-frequency magnetic loss of the soft magnetic composites. The EPMA test results on the surface of the mixed particles show that the phosphoric acid and high-temperature-resistant silicone resin contain Si, P, and O elements uniformly distributed on the surface of the particles, which indicates that the insulation coating effect is good and uniformly forms an insulation layer on the surface of the powder particles. The magnetic loss of the soft magnetic composite material prepared before and after insulation coating under the conditions of magnetic induction intensity of 20mT and 1 MHz were 554.13 kW/m<sup>3</sup> and 474.36 kW/m<sup>3</sup>, respectively. This indicates that

insulation coating can effectively reduce the loss of soft magnetic composite materials.

Figure 3 shows the XPS results of Fe–Si–B and Fe–Si–B/ferric carbonyl hybrid powder coatings. Figure 3a shows the presence of Fe, O, P, Si, and B elements on the surface of the powder particles after the insulating coating. The addition of different mass fractions of carbonyl iron powder had no effect on the surface elements of the hybrid particles after coating. The detailed information of each element is shown in Fig. 3b–f [14, 15], which shows that the addition of carbonyl iron powder has no negative effect on the insulation coating effect of the hybrid particles. Referring to Figs. 1, 2, and 3, the carbonyl iron powder effectively filled the voids between the large particles and the insulating coating process formed a relatively uniform insulating coating layer on the surface of the particles.

The VSM detection results of Fe–Si–B and Fe–Si–B/carbonyl iron hybrid particles after insulation coating are shown in Fig. 4a. The hysteresis lines of the five groups of powder particles after insulation cladding were tested with a vibrating sample magnetometer, and the test results showed that the saturation magnetization intensity of the powder particles increased with the increase of the mass proportion of carbonyl iron powder. The saturation magnetization intensity of the powder particles directly affects the high-frequency performance of the soft magnetic composites. The high-frequency performance of the soft magnetic composites was enhanced with the increase of the saturation magnetization intensity of the magnetic powder. With the increase of the mass ratio of carbonyl iron powder, the magnetization intensities of the five groups of powder particles at 1 T magnetic field were 166.84 emu/g, 171.55 emu/g, 176.09 emu/g, 176.81 emu/g, and 185.39 emu/g, respectively. The coercivity and remanence of the mixed powder particles hardly changed with the increase of the mass ratio of carbonyl iron powder, maintaining the excellent soft magnetic properties, as shown in Fig. 4b.

In order to research the effects of Carbonyl iron additives on the molding process of soft magnetic composite materials, the density of soft magnetic composite materials was detected, and the test results are shown in Table 1. The density of soft magnetic composites increases with the increase of carbonyl iron additive content, which indicates that carbonyl iron additive can significantly reduce the interaction

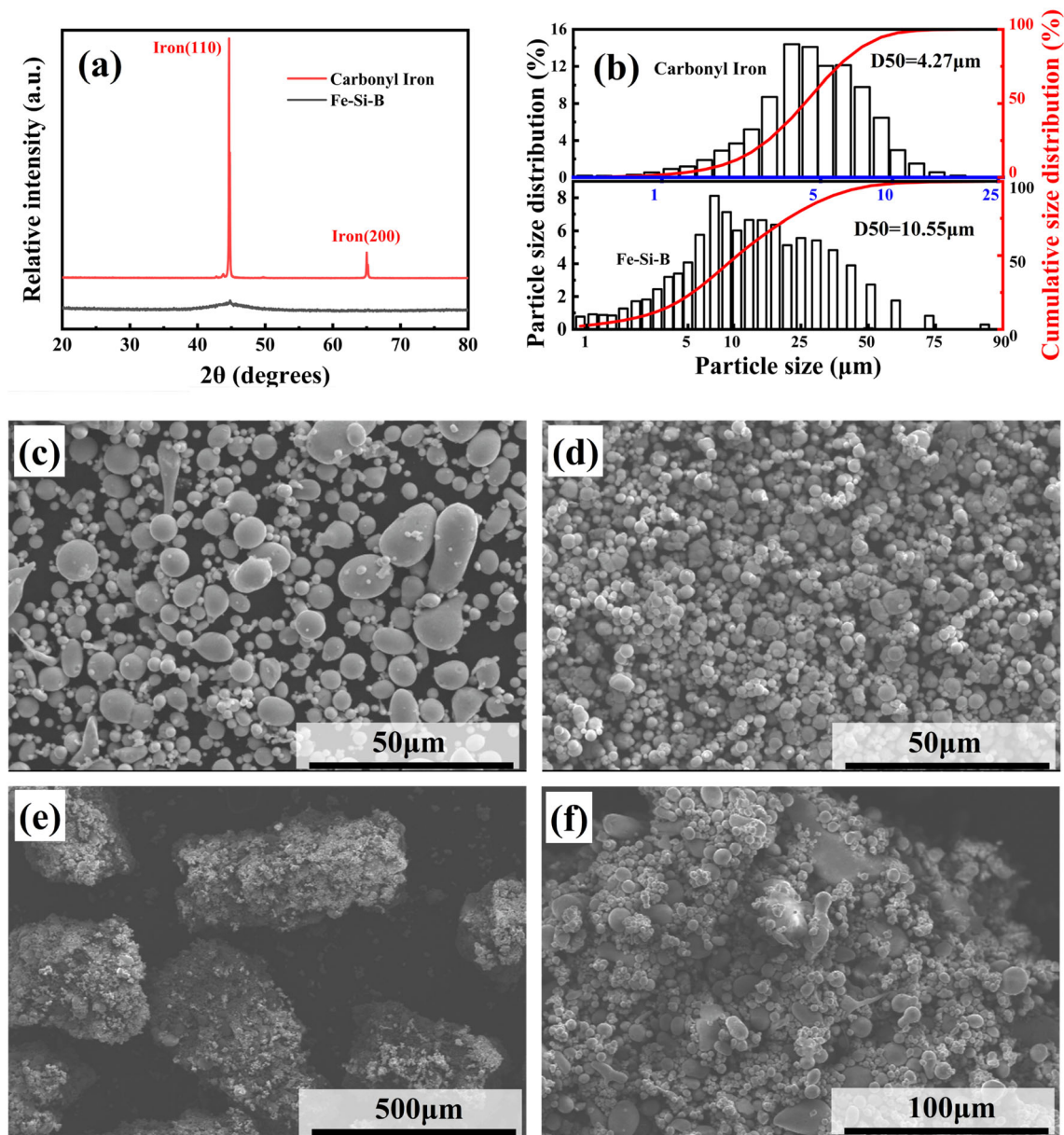


**Fig. 1** **a** XRD results of carbonyl iron and Fe-Si-B powders, **b** Particle size distribution of carbonyl iron and Fe-Si-B powders (c) and **d** Morphology of Fe-Si-B amorphous powder and

carbonyl iron powder (e) and **f** Morphology of Fe-Si-B/carbonyl iron-mixed powder after granulation

force between Fe-Si-B amorphous particles during the compression of soft magnetic composites. During the compression molding process, the carbonyl iron additive not only fills the voids between the particles, but also acts as a lubricant to reduce the friction between the particles and prevent the insulation coating from peeling off. The density of soft magnetic composites is also one of the important factors affecting their magnetic properties. The increase in density leads to the reduction of voids inside the soft

magnetic composites, which can significantly increase the magnetic permeability of soft magnetic composites [16–19]. The microstructure of soft magnetic composites was photographed to investigate more visually the effect of carbonyl iron additives on the density of soft magnetic composites. Figure 5 shows the microstructure of the soft magnetic composites with carbonyl iron content of 0wt% and 25wt%, respectively. It can be seen from the figure that the soft magnetic composites without

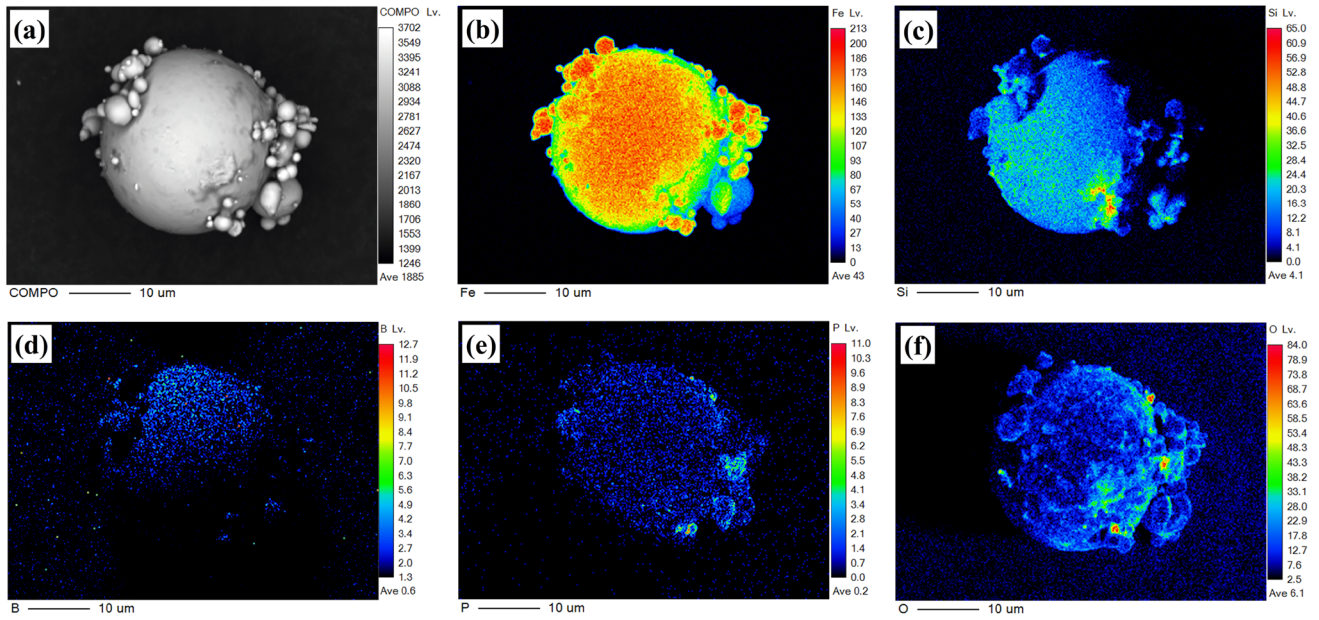


Fig. 2 EPMA test results on the surface of powder particles after insulation coating a Original particles, b Fe, c Si, d B, e P, and f O

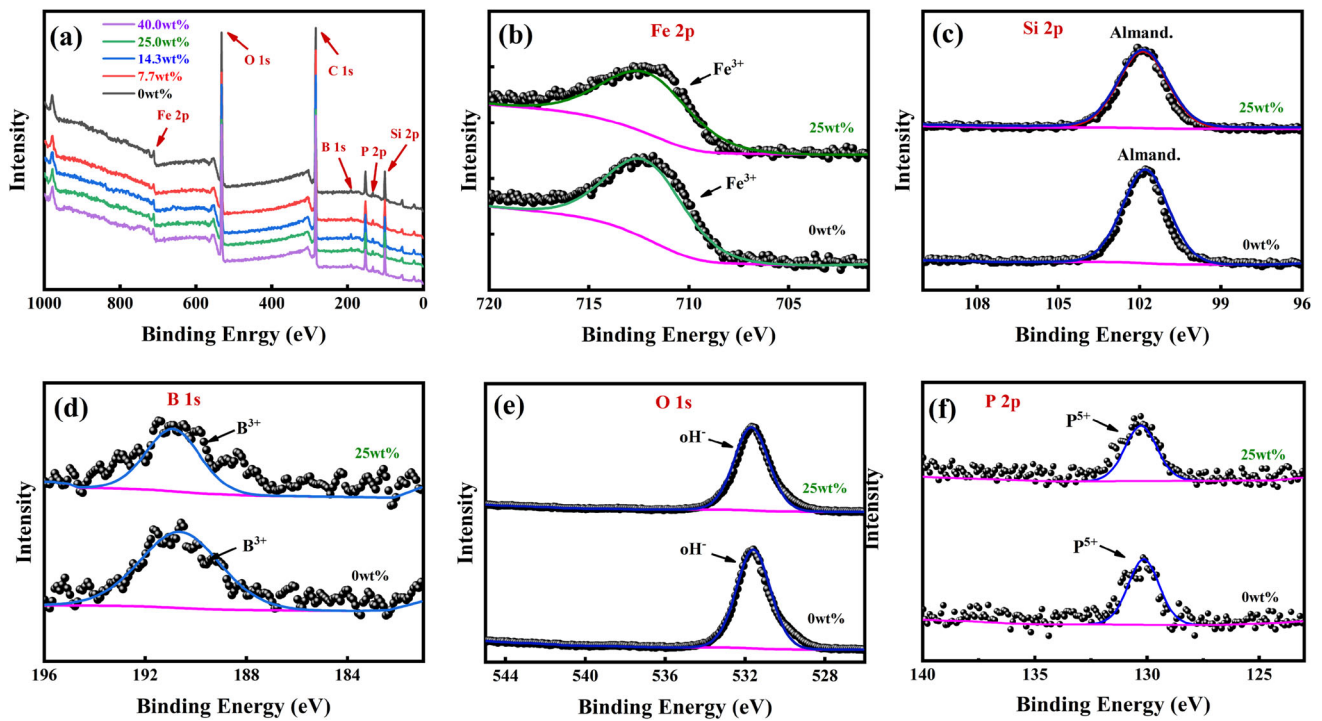
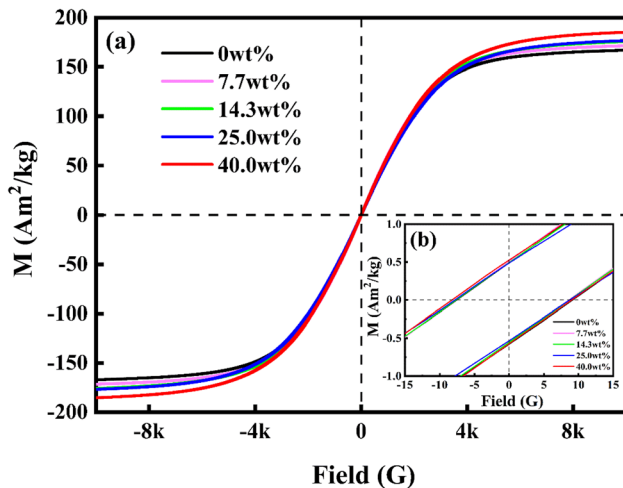


Fig. 3 a XPS full spectrum detection results of Fe–Si–B/carbonyl iron-mixed powder particles after adding different mass fractions of carbonyl iron powder, b Fe2p, c Si2p, d B1s, e O1s, and f P2p

carbonyl iron additives have almost no deformation of the internal particles, which makes it possible that there are more voids between the particles and is the reason for their low density. The soft magnetic

composites with carbonyl iron additives contain a large number of deformed carbonyl iron particles, which leads to a significant increase in the density of the soft magnetic composites.



**Fig. 4** Hysteresis loops of Fe-Si-B/carbonyl iron-mixed powder particles after adding carbonyl iron particles with different mass fractions

In order to further research the properties of Fe-Si-B/carbonyl iron soft magnetic composites, the iron loss and relative permeability of Fe-Si-B/carbonyl iron soft magnetic composites were tested under different magnetic induction magnitude  $B_m$  and magnetic field frequencies. The relative magnetic permeability of Fe-Si-B/carbonyl iron soft magnetic composites at different frequencies when the magnetic induction strength is 50 mT is shown in Fig. 6a. The magnetic permeability of the soft magnetic composites was significantly increased by about 25% with the increase of the proportion of carbonyl iron powder. In addition, the relative permeability test results show that the relative permeability of the soft

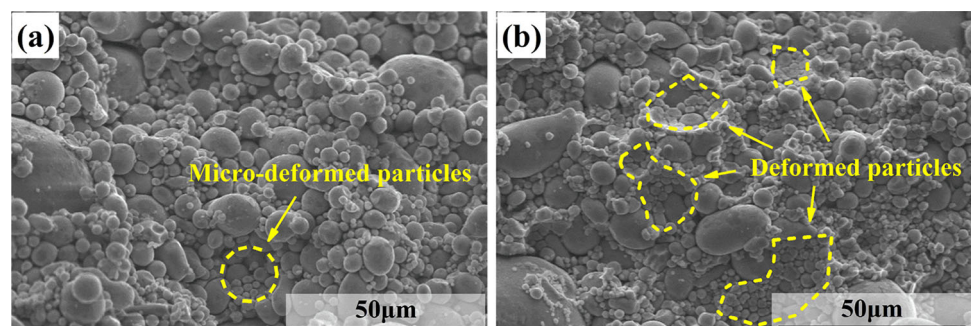
magnetic composites has excellent stability. The relative magnetic permeability of the soft magnetic composites fluctuated within a small range with the change of magnetic field frequency. The iron loss of Fe-Si-B/carbonyl iron soft magnetic composites at different frequencies is shown in Fig. 6c. Magnetic field frequency is an important factor affecting the iron loss of soft magnetic composites. The iron loss of soft magnetic composites also increases rapidly with the increase of magnetic field frequency, and the addition of carbonyl iron powder particles has a subtle effect on the iron loss of soft magnetic composites below 1 M frequency. Under the same conditions, the iron loss of soft magnetic composites decreases with the increase of carbonyl iron content.

The relative permeability and iron loss of the soft magnetic composites were tested at a magnetic induction strength of 20 mT at high-frequency magnetic fields. The test results showed that the relative magnetic permeability of Fe-Si-B/carbonyl iron soft magnetic composites still had excellent stability under high-frequency magnetic fields, as shown in Fig. 6b. With the increase of the weight ratio of carbonyl iron powder particles, the iron loss of Fe-Si-B/carbonyl iron soft magnetic composites under high-frequency magnetic field significantly decreased, indicating that the addition of carbonyl iron powder particles reduced the iron loss of soft magnetic composites at high frequency. When the mass proportion of carbonyl iron powder particles is greater than 25%, the decreasing trend of iron loss of soft magnetic composites becomes slow, as shown in Fig. 6d. The iron losses of the five groups of samples

**Table 1** Density of soft magnetic composites with different carbonyl iron additive contents ( $\text{g}/\text{cm}^3$ )

Content	0wt%	7.7wt%	14.3wt%	25.0wt%	40.0wt%
Density	$6.178 \pm 0.022$	$6.321 \pm 0.092$	$6.485 \pm 0.024$	$6.708 \pm 0.026$	$6.920 \pm 0.019$

**Fig. 5** Microstructures of the soft magnetic composites with carbonyl iron content of 0wt% and 25wt%. **a** 0wt% and **b** 25wt%



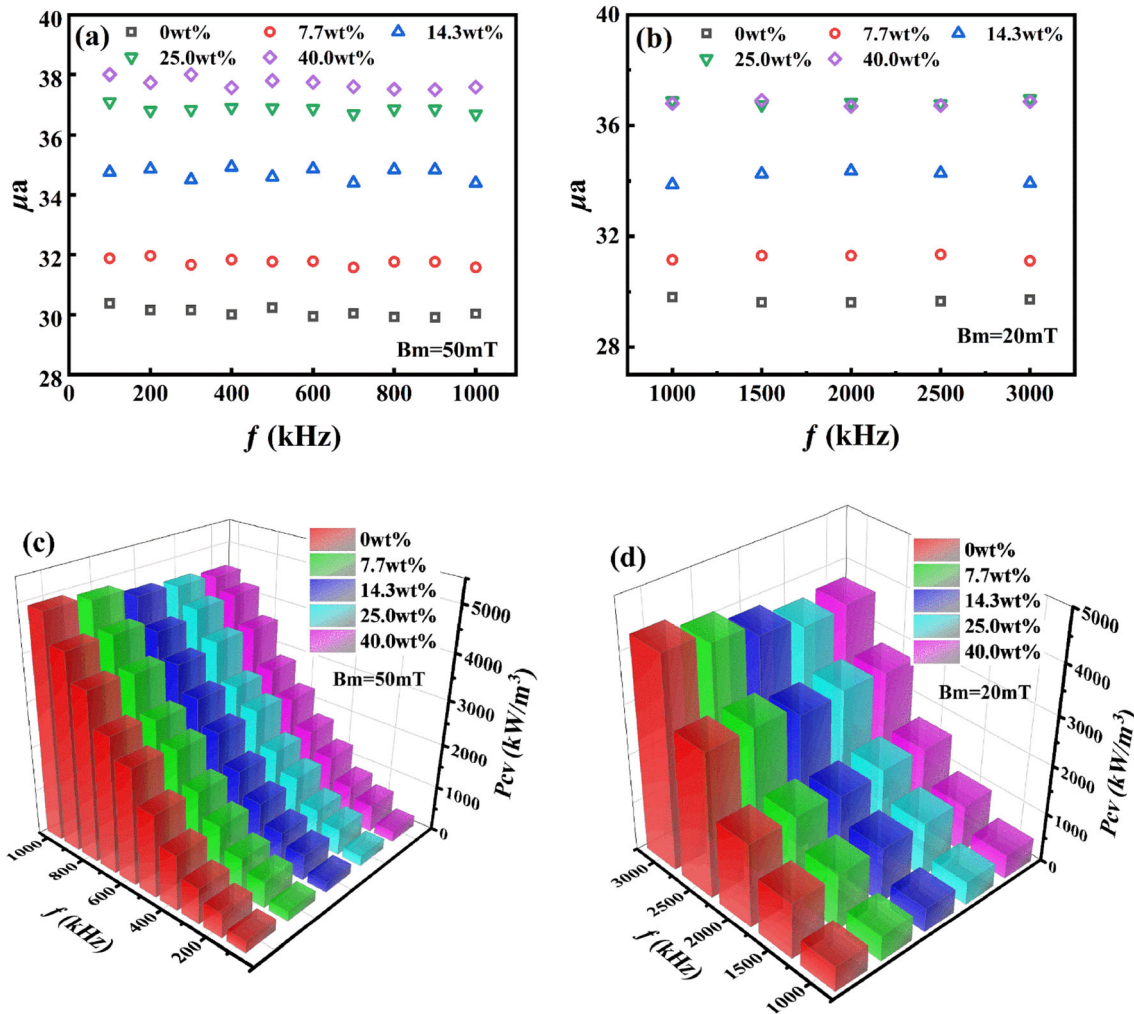


**Fig. 6** a and b Relative permeability as function of magnetic field for Fe-Si-B/carbonyl iron soft magnetic composites with different carbonyl iron contents measured at 50 and 20 mT. c and d The

at 1 MHz magnetic field frequency are 521.51  $\text{kW/m}^3$ , 519.33  $\text{kW/m}^3$ , 495.53  $\text{kW/m}^3$ , 474.36  $\text{kW/m}^3$ , and 492.98  $\text{kW/m}^3$ , respectively, which are lower than the values reported in the literature [7, 20, 21].

In general, the iron loss of soft magnetic composites is the result of the combined effect of hysteresis loss and dynamic loss. Hysteresis loss ( $P_h$ ) as the loss due to hysteresis behavior can be obtained by calculating the area of the hysteresis loop. Hysteresis loss can usually be expressed by Eq. 1. The dynamic loss mainly includes the eddy current loss between particles ( $P_{ed}^{inter}$ ), the eddy current loss inside the particle ( $P_{ed}^{intra}$ ), and the residual loss ( $P_r$ ) [22–26]. They can be expressed as follows:

magnetic loss of the soft magnetic composite varies with the content of carbonyl iron and frequency at  $B_m = 50$  mT and 20 mT

$$P_h = f \oint HdB, \tag{1}$$

where  $f$  is the frequency,  $H$  is the magnetic field, and  $B$  is the magnetic induction.

$$P_{ed}^{inter} = \frac{(\pi d_{eff} B_m)^2}{\beta \rho_{SMCs}} f^2, \tag{2}$$

$$P_{ed}^{intra} = \frac{(\pi d_{FC} B_m)^2}{\beta \rho_{FC}} f^2, \tag{3}$$

$$P_r = \frac{16GSB_m^2}{n_0 \rho_{FC}} f^2, \tag{4}$$

where  $d_{eff}$  is the effective diameter of eddy current which can be regarded as the thickness of the Fe–Si–B/carbonyl iron soft magnetic composites,  $\beta$  is the geometric coefficient,  $d_{FC}$  is the diameter of the Fe–Si–B/carbonyl iron particles,  $\rho_{SMCs}$  is the resistivity of the soft magnetic composite,  $\rho_{FC}$  is the resistivity of the Fe–Si–B/carbonyl iron particles,  $G$  is the dimensionless coefficient,  $S$  is the cross section of the Fe–Si–B/carbonyl iron soft magnetic composites perpendicular to the magnetic flux direction, and  $n_0$  is the number of active domain walls. The iron losses of the soft magnetic composites under different magnetic field conditions were separated by a nonlinear fitting method, and the data obtained are shown in Fig. 7. It can be seen from Fig. 7a and b that the hysteresis loss and dynamic loss of the soft magnetic composites vary with the increase of the carbonyl iron additive content. The increase in carbonyl iron content leads to a rise in hysteresis loss and a decrease in dynamic loss in soft magnetic composites. The dynamic loss of soft magnetic composites is highly sensitive to

magnetic field frequency and magnetic induction magnitude, and the dynamic loss increases rapidly with the increase of magnetic induction magnitude and magnetic field frequency. However, the dynamic loss of Fe–Si–B/carbonyl iron soft magnetic composites at high frequencies shows a decreasing trend with the increase of carbonyl iron additive content, as shown in Fig. 7d. Soft magnetic composites have severe eddy current effects at high frequencies. Although the small voids inside the soft magnetic composites help reduce eddy current losses, a high resistivity insulating cladding can reduce eddy current losses more effectively. The use of carbonyl iron powder particles with D50 of 4.27  $\mu\text{m}$  mixed with large particle size Fe–Si–B can fill the gaps between large powder particles. The presence of carbonyl iron powder enhances the coupling between the particles and contributes to less eddy current loss at high frequencies. Meanwhile, the insulating coating on the surface of the particles within the high-density soft

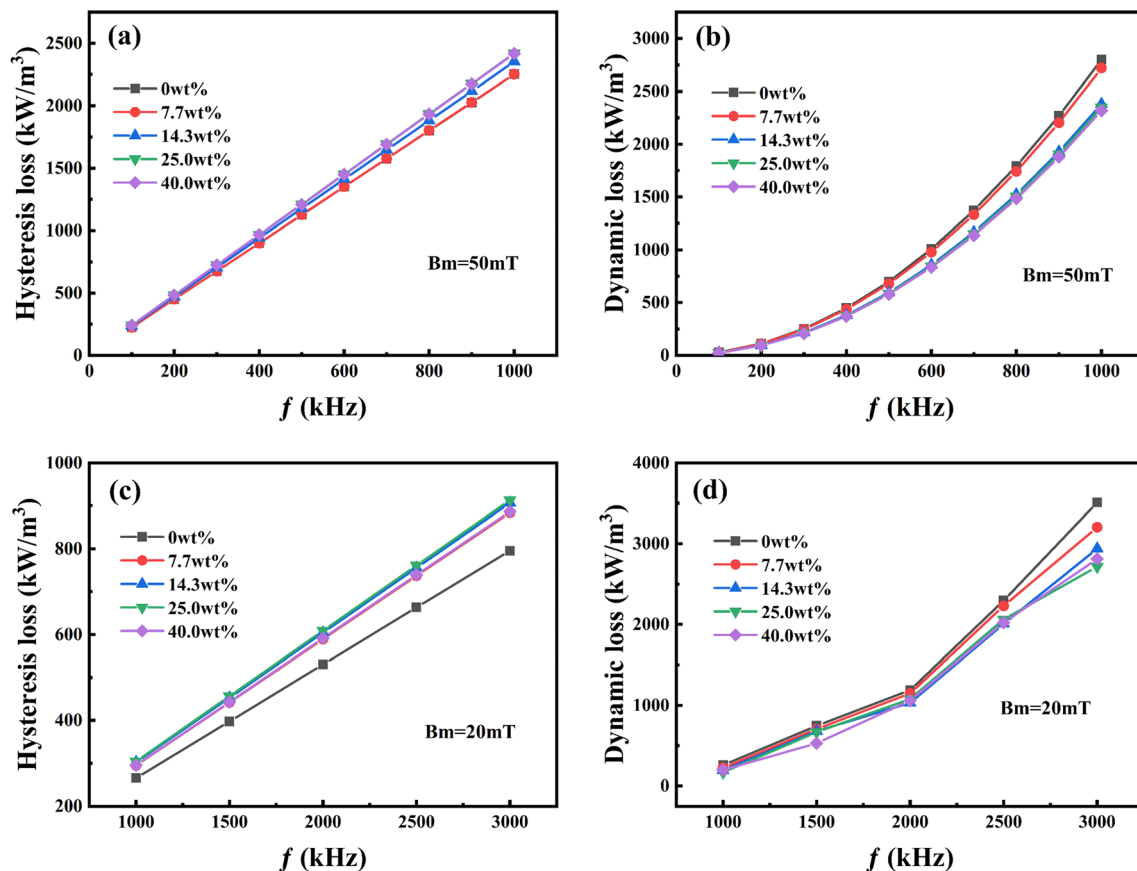


**Fig. 7** Different frequency at 50 mT and 20mT for different carbonyl iron contents Fe–Si–B/carbonyl iron soft magnetic composites with loss separation including (a)/(b) hysteresis loss and (c)/(d) dynamic loss



magnetic composite can effectively reduce the effect of eddy current effect at high frequencies.

The relative permeability and iron loss of Fe–Si–B/carbonyl iron soft magnetic composites were tested at five temperature points of 25 °C, 50 °C, 75 °C, 100 °C, and 125 °C at different magnetic induction magnitude to research the temperature stability of Fe–Si–B/carbonyl iron soft magnetic composites, and the results are shown in Fig. 8. The magnetic permeability of the soft magnetic composites increased slightly with the increase of the test temperature, and accordingly, the iron loss of the soft magnetic composites decreased slightly with the increase of the temperature. The analysis of the relative permeability and iron loss test results of Fe–Si–B/carbonyl iron soft magnetic composites over a wide temperature range shows that the Fe–Si–B/carbonyl iron soft magnetic composites have a low temperature dependence in the temperature range of 25 to 125 °C. Meanwhile, the relative permeability and iron loss of the soft magnetic composites remain excellent at higher temperatures compared to room temperature.

The above mentioned that the addition of carbonyl iron additives will improve the high-frequency performance of soft magnetic composites. To verify this claim, the complex permeability tests were performed for Fe–Si–B/carbonyl iron soft magnetic composites with different carbonyl iron contents below 100 MHz with frequency variation, and the results are shown in Fig. 9. It can be seen from Fig. 9 that the real part  $\mu'$  of the complex permeability of the soft magnetic composite material has good high-

frequency stability below 10 MHz. The permeability of soft magnetic composites increased from 30 to about 38 with the increase of carbonyl iron additive content. The imaginary part  $\mu''$  of the complex permeability of Fe–Si–B/carbonyl iron soft magnetic composites in Fig. 9 also has excellent high-frequency stability in the range of 0.1 to 10 MHz, and the content of carbonyl iron additives has almost no effect on it. When the frequency is 1 MHz, the corresponding imaginary parts  $\mu''$  of the soft magnetic composites with 0 wt%, 7.7 wt%, 14.3 wt%, 25.0 wt%, and 40.0 wt% of carbonyl iron additives are about 0.092, 0.106, 0.115, 0.125, and 0.128, respectively, which are much smaller than the values reported in Refs [27–29],

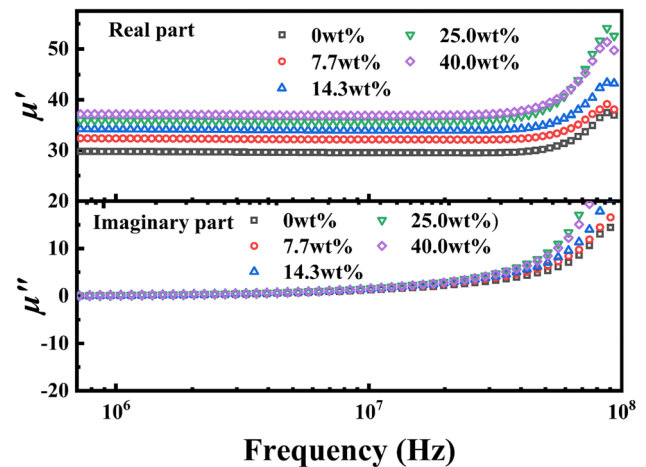


Fig. 9 Complex permeability of Fe–Si–B/carbonyl iron soft magnetic composites with different carbonyl iron contents below 100 MHz

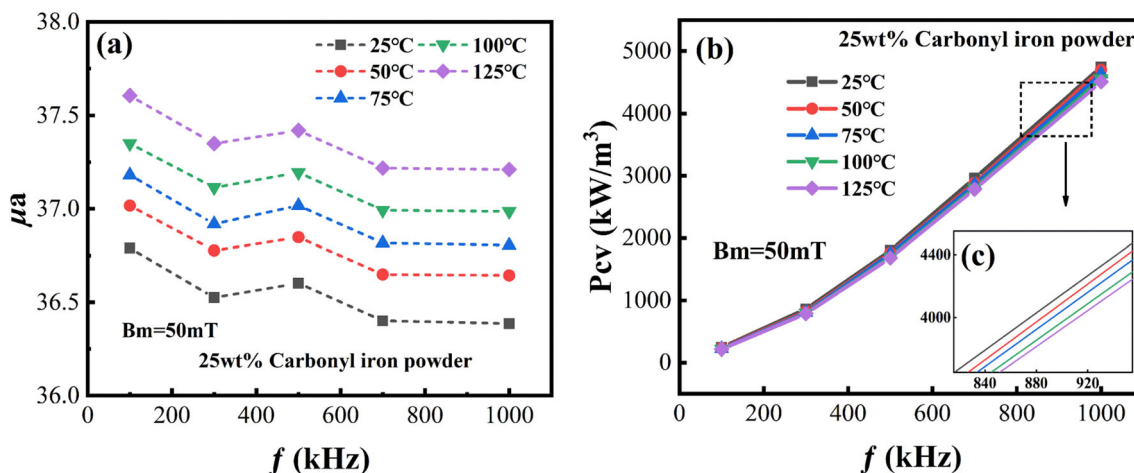


Fig. 8 Relative permeability and iron loss of Fe–Si–B/carbonyl iron soft magnetic composites at different temperatures and external magnetic fields (25wt% carbonyl iron)

indicating that the soft magnetic composites have a lower magnetic loss at high frequencies and are suitable for high-frequency devices. The results in Fig. 9 also show that the cutoff frequency  $f_r$  is well above 50 MHz for all Fe–Si–B/carbonyl iron soft magnetic composites, so the residual loss caused by the positive and negative transformation of the high-frequency magnetic field can be ignored.

In this study, the magnetic property characterization of annular soft magnetic composite samples is an important step in the development of power inductors. On the premise of reducing the magnetic loss of soft magnetic composites as much as possible, different types of power inductors can be designed based on the permeability of soft magnetic composites to meet the different requirements of integrated circuits.

## 4 Conclusions

In summary, a novel method of preparing high-frequency Fe–Si–B/carbonyl iron soft magnetic composites with low iron loss characteristics by adding carbonyl iron powder with high-saturation magnetization intensity is proposed. The saturation magnetization intensity of Fe–Si–B/carbonyl iron hybrid powder particles increases with the increase of mass fraction of carbonyl iron powder. The density of the soft magnetic composites increased with the increase of the mass ratio of carbonyl iron powder. SEM images of soft magnetic composites show that the filling of small carbonyl iron particles between the voids is an important factor in the increase of density of soft magnetic composites. With the increase of carbonyl iron powder content, the relative permeability and iron loss of Fe–Si–B/carbonyl iron soft magnetic composites were optimized accordingly. The loss separation of the iron loss reveals that the dynamic loss of the soft magnetic composites dominates the loss at high-frequency conditions. Soft magnetic composites fabricated at the same time have sound temperature stability and the temperature variation has less effect on their performance. The results of complex permeability tests show that Fe–Si–B/carbonyl iron soft magnetic composites have excellent high-frequency stability. This study has potential commercial value in the research and development application of high-frequency power electronic devices.

## Author contributions

All authors contributed to the study conception and design. Material preparation, data collection, and analysis were performed by BW, LC, LL, CZ, BW, YT, YY, JD, and GW. The first draft of the manuscript was written by JS, and all authors commented on previous versions of the manuscript. All authors read and approved the final manuscript.

## Funding

This work was funded by the by the Natural Science Foundation of Liaoning Province of China (2020-MS-078) and the Fundamental Research Funds for the Central Universities (N2007009).

## Data availability

All data generated or analyzed during this study are included in this published article.

## Declarations

**Competing interests** The authors have no relevant financial or non-financial interests to disclose.

## References

1. J.M. Silveyra, E. Ferrara, D.L. Huber, T.C. Monson, *Science* **362**(6413), eaao0195 (2018). <https://doi.org/10.1126/science.aao0195>
2. O. Gutfleisch, M.A. Willard, E. Bruck, C.H. Chen, S.G. Sankar, J.P. Liu, *Adv. Mater.* **23**(7), 821–42 (2011). <https://doi.org/10.1002/adma.201002180>
3. Z. Akase, K. Kimura, T. Saito, K. Niitsu, T. Tanigaki, Y. Iwasaki, P. Sharma, A. Makino, D. Shindo, *J. Magn. Magn. Mater.* **541**, 168519 (2022). <https://doi.org/10.1016/j.jmmm.2021.168519>
4. N.V. Ilin, S.V. Komogortsev, G.S. Kraynova, A.V. Davydenko, I.A. Tkachenko, A.G. Kozlov, V.V. Tkachev, V.S. Plotnikov, *J. Magn. Magn. Mater.* **541**, 168525 (2022). <https://doi.org/10.1016/j.jmmm.2021.168525>

5. K. Lu, X. Liu, J. Wang, T. Yang, J. Xu, J. Alloys Compd. **892**, 162100 (2022). <https://doi.org/10.1016/j.jallcom.2021.162100>
6. S. Mori, T. Mitsuoka, K. Sugimura, R. Hirayama, M. Sonehara, T. Sato, N. Matsushita, Adv. Powder Technol. **29**(6), 1481–1486 (2018). <https://doi.org/10.1016/j.apt.2018.03.012>
7. N. Yabu, K. Sugimura, M. Sonehara, T. Sato, IEEE Trans. Magn. **54**(11), 1–5 (2018). <https://doi.org/10.1109/TMAG.2018.2832662>
8. J.L. Ni, F. Duan, S.J. Feng, F. Hu, X.C. Kan, X.S. Liu, J. Alloys Compd. **897**, 163191 (2022). <https://doi.org/10.1016/j.jallcom.2021.163191>
9. C. Liu, A. Inoue, F.L. Kong, E. Zanaeva, A. Bazlov, A. Churyumov, S.L. Zhu, F.A. Marzouki, R.D. Shull, J. Non-Crystalline Solids **554**, 120606 (2021). <https://doi.org/10.1016/j.jnoncrysol.2020.120606>
10. K.L. Alvarez, H. Ahmadian Baghbaderani, J.M. Martín, N. Burgos, P. McCloskey, J. González, A. Masood, J. Non-Crystalline Solids **574**, 121151 (2021). <https://doi.org/10.1016/j.jnoncrysol.2021.121151>
11. Y. Dong, Z. Li, M. Liu, C. Chang, F. Li, X.-M. Wang, Mater. Res. Bull. **96**, 160–163 (2017). <https://doi.org/10.1016/j.materresbull.2017.04.030>
12. Y.J. Li, Y.G. Wang, B. An, H. Xu, Y. Liu, L.C. Zhang, H.Y. Ma, W.M. Wang, PLoS One **11**(1), e1046421 (2016). <https://doi.org/10.1371/journal.pone.0146421>
13. T. Wang, X. Bian, C. Yang, S. Zhao, M. Yu, Appl. Surf. Sci. **399**, 663–669 (2017). <https://doi.org/10.1016/j.apsusc.2016.12.145>
14. H. Zhang, Z.C. Yan, Q. Chen, Y. Feng, Z.G. Qi, H.Z. Liu, X.Y. Li, W.M. Wang, J. Non-Crystalline Solids **564**, 120830 (2021). <https://doi.org/10.1016/j.jnoncrysol.2021.120830>
15. Y. Fan, S. Zhang, X. Xu, J. Miao, W. Zhang, T. Wang, C. Chen, R. Wei, F. Li, Intermetallics **138**, 107306 (2021). <https://doi.org/10.1016/j.intermet.2021.107306>
16. J. Wang, X.A. Fan, Z. Wu, G. Li, J. Solid State Chem. **231**, 152–158 (2015). <https://doi.org/10.1016/j.jssc.2015.08.016>
17. C. Wu, X. Gao, G. Zhao, Y. Jiang, M. Yan, J. Magn. Mater. **452**, 114–119 (2018). <https://doi.org/10.1016/j.jmmm.2017.12.032>
18. R.R. Bai, Z.H. Zhu, H. Zhao, S.H. Mao, Q. Zhong, J. Magn. Mater. **433**, 285–291 (2017). <https://doi.org/10.1016/j.jmmm.2017.03.016>
19. H.J. Liu, H.L. Su, W.B. Geng, Z.G. Sun, T.T. Song, X.C. Tong, Z.Q. Zou, Y.C. Wu, Y.W. Du, J. Supercond. Nov. Magn. **29**, 463–468 (2016). <https://doi.org/10.1007/s10948-015-3282-4>
20. C. Xia, Y. Peng, X. Yi, Z. Yao, Y. Zhu, G. Hu, J. Non-Crystalline Solids (2021). <https://doi.org/10.1016/j.jnoncrysol.2021.120673>
21. H.-R. Kim, M.-S. Jang, Y.-G. Nam, Y.-S. Kim, S.-S. Yang, Y.-J. Kim, J.-W. Jeong, Metals **11**, 1220 (2021). <https://doi.org/10.3390/met11081220>
22. H. Shokrollahi, K. Janghorban, J. Mater. Process. Technol. **189**(1–3), 1–12 (2007). <https://doi.org/10.1016/j.jmatprotec.2007.02.034>
23. E.A. Périgo, B. Weidenfeller, P. Kollár, J. Füzér, Appl. Phys. Rev. **5**, 031301 (2018). <https://doi.org/10.1063/1.5027045>
24. P. Kollár, D. Olekšáková, V. Vojtek, J. Füzér, M. Fáberová, R. Bureš, J. Magn. Mater. **424**, 245–250 (2017). <https://doi.org/10.1016/j.jmmm.2016.10.060>
25. P. Kollár, Z. Birčáková, J. Füzér, R. Bureš, M. Fáberová, J. Magn. Mater. **327**, 146–150 (2013). <https://doi.org/10.1016/j.jmmm.2012.09.055>
26. Z. Luo, X.a. Fan, Y. Zhang, Z. Yang, J. Wang, Z. Wu, X. Liu, G. Li, Y. Li, Adv. Powder Technol. **32**(9), 3364–3371 (2021). <https://doi.org/10.1016/j.apt.2021.07.024>
27. J.L. Ni, F. Hu, S.J. Feng, X.C. Kan, Y.Y. Han, X.S. Liu, J. Alloys Compd. **887**, 161337 (2021). <https://doi.org/10.1016/j.jallcom.2021.161337>
28. M. Strečková, L. Medvecký, J. Füzér, P. Kollár, R. Bureš, M. Fáberová, Mater. Lett. **101**, 37–40 (2013). <https://doi.org/10.1016/j.matlet.2013.03.067>
29. F. Hu, J.L. Ni, S.J. Feng, X.C. Kan, R.W. Zhu, W. Yang, Y.J. Yang, Q.R. Lv, X.S. Liu, J. Magn. Mater. **501**, 166480 (2020). <https://doi.org/10.1016/j.jmmm.2020.166480>

**Publisher's Note** Springer Nature remains neutral with regard to jurisdictional claims in published maps and institutional affiliations.

Springer Nature or its licensor (e.g. a society or other partner) holds exclusive rights to this article under a publishing agreement with the author(s) or other rightsholder(s); author self-archiving of the accepted manuscript version of this article is solely governed by the terms of such publishing agreement and applicable law.